
Solution and Solid-State Studies of Alkali Metal Aggregate Assemblies

John Jacob Morris

Publication Date

07-04-2008

License

This work is made available under a All Rights Reserved license and should only be used in accordance with that license.

Citation for this work (American Psychological Association 7th edition)

Morris, J. J. (2008). *Solution and Solid-State Studies of Alkali Metal Aggregate Assemblies* (Version 1). University of Notre Dame. <https://doi.org/10.7274/br86b27956f>

This work was downloaded from CurateND, the University of Notre Dame's institutional repository.

For more information about this work, to report or an issue, or to preserve and share your original work, please contact the CurateND team for assistance at curate@nd.edu.

CHAPTER 6

SYSTEMATIC STUDY OF *para*-SUBSTITUTED ALKALI METAL ARYLOXIDE AGGREGATES HIGHLIGHTED BY THEIR INORGANIC CONNECTIVITY

6.1 Introduction

During our targeted synthesis of high-connectivity networks using alkali metal aryloxide aggregates, we studied the viability of using aryloxides substituted at the *para*-position by a halide (Figure 6.1). We were particularly interested in this class of substituted phenols for two reasons: (i) the strongly electron-withdrawing group may promote the formation of smaller aggregates, and (ii) the previously synthesized sodium 4-F-phenoxide dioxane complex, $[(4\text{-F-C}_6\text{H}_4\text{ONa})_6\cdot(\text{dioxane})_3]_\infty$, displayed unique network bonding through Na-F_{Ar} interactions.¹ We became interested in using this type of interaction for other systems as a means of network growth.

All of the lithium 4-X-phenoxide dioxane complexes, where X = F, Cl, Br, I, previously studied by our group formed tetrameric aggregates, with the sodium analogues forming hexameric aggregates without the need for bulky substituents at the *ortho*-position.² For the heavier alkali metals, the lack of a substituent at the *ortho*-position potentially allows for an increase in the number of M-O_{solv} bonds, which could lead to high-connectivity networks when a divergent linker is used.

The network bonding in the previously synthesized sodium 4-F-phenoxide dioxane complex, $[(4\text{-F-C}_6\text{H}_4\text{ONa})_6 \cdot (\text{dioxane})_3]_\infty$, is unique within the set of alkali metal aryloxide systems we have studied.² The complex forms a hexameric aggregate that gives a two-dimensional 4⁴-net through dioxane bridges. However, there are close transannular Na-F_{Ar} interactions between hexameric aggregates, which increases the dimensionality of the extended structure to give a three-dimensional network with primitive cubic (**pcu**) topology. The formation of the Na-F interactions prompted us to further study systems that could have this type of metal-halide interaction. There are two main sections in this chapter. The first highlights the complexes that form extended networks from discreet SBUs, while the second highlights those that form networks from polymeric inorganic rods.

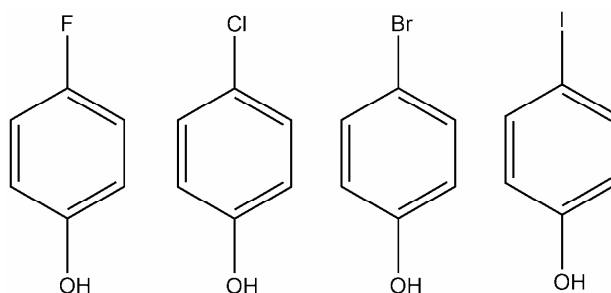


Figure 6.1 *Para*-substituted phenols highlighted in this chapter.

6.1.1 Hybrid Inorganic-Organic Frameworks

As a class of materials, coordination frameworks are a hybrid between purely inorganic extended materials such as aluminosilicates and organic polymers such as polyolefins.³ A definition of a coordination network could therefore be any material that contains both inorganic and organic components as integral parts of a network with infinite bonding in at least one dimension. All of the compounds described so far form

discreet SBUs that are linked by organic ligands. Indeed, a vast majority of coordination networks, whether formed from a single metal center or cluster, fall into this category.⁴ In these materials, the aggregate acts as a zero-dimensional node and the dimensionality of the extended structure is derived from connecting these nodes through organic ligands. Coordination networks can also be constructed from extended inorganic rods or sheets that are connected by polyfunctional organic ligands.³ In these materials, which are called extended inorganic hybrids, one or two of the total dimensions are composed of only M-X-M bonding, where X = O, N, S, F, among others.⁵ An example is shown in Figure 6.2 of a nickel succinate structure, $\text{Ni}_7(\text{OH})_6(\text{H}_2\text{O})_3(\text{C}_4\text{H}_4\text{O}_4)_4 \cdot 7\text{H}_2\text{O}$, in which one-dimensional inorganic chains composed of Ni-O-Ni bonding are cross linked by the organic succinate ligands to give a two-dimensional sheet structure.⁶ Another example is the nickel gallate structure, $\text{Ni}(\text{C}_7\text{O}_5\text{H}_4) \cdot 2\text{H}_2\text{O}$, in which one-dimensional Ni-O-Ni chains are bridged in two-dimensions by the organic gallate ligands to give a three-dimensional structure.⁷

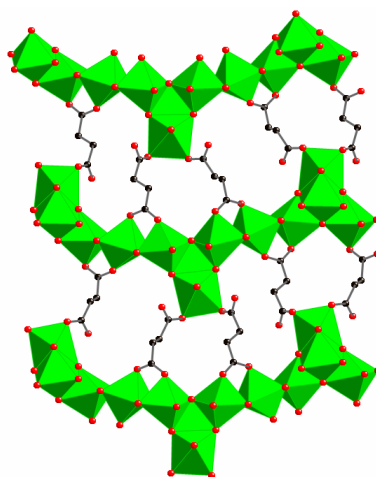


Figure 6.2 The extended structure of nickel succinate containing 1D inorganic chains, bridged by organic ligands along a second dimension to form sheets. NiO_6 octahedra in green with carbon and oxygen as black and red sphere, respectively.

A classification system has been developed to describe extended structures in terms of the dimensionality of their inorganic and organic connectivities. The classification uses the nomenclature I^xO^y where I = inorganic, O = organic, x = dimensionality of the inorganic connectivity, y = dimensionality of the organic connectivity, and the sum of the exponents gives the overall dimensionality of the structure. Depending on the dimensionality of the structure I = 0-3 and O = 0-3. A complex such as the 4⁴-net $[\{(2-t\text{Bu-C}_6\text{H}_4\text{OK})_6\supset(\text{H}_2\text{O})\}\cdot(\text{dioxane})_4]_\infty$, **5.1**, described in the previous chapter would be classified as I^0O^2 , whereas the 3D diamondoid network $[\{[(2-t\text{Bu-C}_6\text{H}_4\text{ORb})_6\supset(\text{H}_2\text{O})]\cdot(\text{dioxane})_4\}\cdot(\text{dioxane})]_\infty$, **5.3**, would be classified as I^0O^3 . In both structures, a hexameric molecular aggregate is formed (I^0) and the resulting extended structure is based solely on the organic ligands. The two-dimensional structure, **5.1**, is therefore I^0O^2 , and the three-dimensional structure, **5.3**, is I^0O^3 . Using the transition metal examples described above, the nickel succinate structure is classified I^1O^1 , since the two-dimensional structure has one dimension each of inorganic and organic connectivity, whereas the three-dimensional nickel gallate structure is I^1O^2 . A structure with classification I^3O^0 would be a completely inorganic structure, whereas a structure with I^0O^3 would be an extended structure with only organic connectivity. This classification system is not meant as a substitute for other systems, such as Schläfli symbols, but rather as a way to readily identify extended materials that have a mixture of extended inorganic and organic components. Complexes from our own group with this type of connectivity will be highlighted in the final section of this chapter (Section 6.3).

6.2 Coordination Frameworks From Discreet SBUs

6.2.1 Synthesis

The equimolar reaction of 4-F-phenol with KHMDS in 1,4-dioxane resulted in the instant formation of a precipitate, which dissolved on vigorous heating. High-quality crystals of $[(4\text{-F-C}_6\text{H}_4\text{OK})_6\cdot(\text{dioxane})_4]_\infty$ (**6.1**) were grown from the reaction solution after optimizing the concentration and temperature for crystal growth. Subsequent equimolar reactions of 4-I-phenol with KHMDS or $[\text{RbOBu}^t\cdot\text{Bu}^t\text{OH}]_\infty$ under similar crystallization conditions gave high-quality crystals of $[(4\text{-I-C}_6\text{H}_4\text{OK})_6\cdot(\text{dioxane})_6]_\infty$ (**6.2**) and $[(4\text{-I-C}_6\text{H}_4\text{ORb})_6\cdot(\text{dioxane})_6]_\infty$ (**6.3**).

6.2.2 Molecular Structures

The aggregate of $[(4\text{-F-C}_6\text{H}_4\text{OK})_6\cdot(\text{dioxane})_4]_\infty$, **6.1**, is composed of a hexameric potassium aryloxide aggregate coordinated by eight dioxane molecules (Figure 6.3). The formation of the hexameric aggregate was expected because all of the sodium aryloxides substituted at the *para*-position by halides formed hexameric aggregates.¹ There are three different potassium bonding environments within the aggregate. The first, K1 and its symmetry equivalent, are coordinated by two dioxane molecules as well as a fluoride atom from a neighboring aggregate. As mentioned in the introduction, the sodium 4-F-aryloxide analogue also has a short Na-F_{Ar} distance of 2.5449 (7) Å. The K1-F_{Ar} distance in **6.1** is 2.7385(7) Å, which is well within the K-O_{Diox} distances in **6.1** of 2.7021(8) – 2.7656(9). A list of important bond lengths and angles is reported in Table 6.1. A survey of the CSD shows there are 62 structures that have close K-F distances, which range

between 2.544 - 3.393 Å with a mean of 2.845 Å.⁸ The K1-F_{Ar} distance in **6.1** is therefore on the shorter end of this range. The second potassium, K2, which is the metal in the middle of the hexameric aggregate, is coordinated by only one dioxane. This is the same bonding that was seen in the sodium analogue. The third potassium, K3, is coordinated by one dioxane molecule as well as one fluoride from a neighboring aggregate. The K3-F_{Ar} distance for this potassium is 2.7948(7) Å. In the sodium analogue, the equivalent sodium metal is only coordinated by one dioxane molecule. Both F1 and F2 in the aggregate, and their symmetry equivalents, bridge to neighboring aggregates. In the sodium analogue, only the two fluorides in the middle of the aggregate act as bridges to other aggregates.

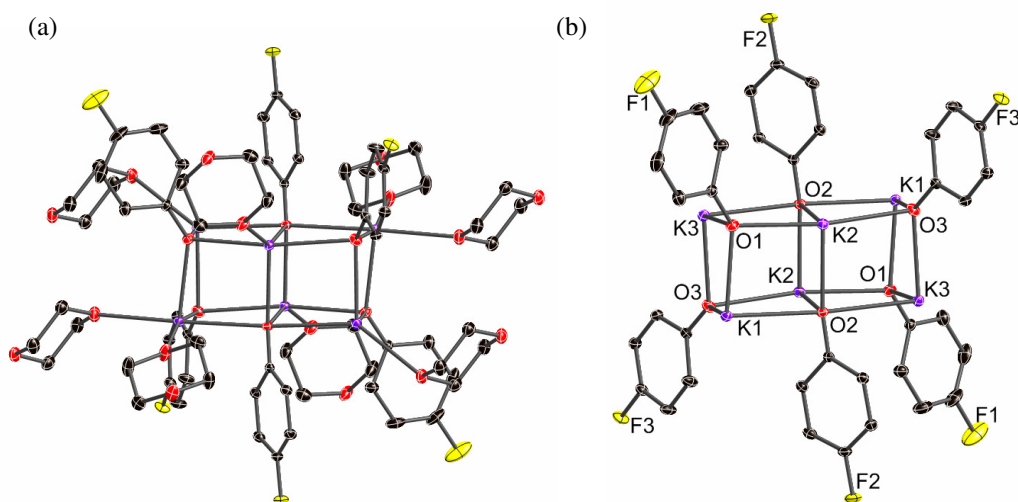


Figure 6.3 Structure of **6.1** showing (a) the full hexameric aggregate with eight coordinated dioxane molecules, and (b) the hexameric aggregate with dioxane molecules removed for clarity.

The potassium and rubidium aggregates of the iodo-substituted phenoxide, [(4-I-C₆H₄OK)₆·(dioxane)₆]_∞ (**6.2**) and [(4-I-C₆H₄ORb)₆·(dioxane)₆]_∞ (**6.3**), are isostructural so only **6.2** is discussed in this section.

Potassium 4-I-phenoxide dioxane, **6.2**, forms a hexameric triple-stack of dimers aggregate coordinate by dioxane, similar to **6.1** (Figure 6.4). However, there are two major differences between the molecular structures. The first is that two of the outer edges of the hexameric aggregate of **6.2** have opened up. The two K3-O3 distances in the aggregate are 4.011 Å, whereas the rest of the K-O_{Ar} distances are 2.623(1) – 2.895(1) Å with a mean of 2.711 Å. It is unclear why it is energetically favorable for these two edges to open, although the difference in energy between the open and closed forms may be quite small. In our previous work, the center of the aryloxide aggregate readily opens, forming the prismatic hexamer, to accommodate increased sterics (or encapsulate water) with no energetic penalty.¹ An argument for the decrease of steric hindrance between aryloxide ligands could be made for the formation of **6.2**, but K3 is coordinated by three dioxane molecules. The potassium should highly favor a close interaction with the anionic aryloxide oxygen over coordination by an additional dioxane molecule. However, this is the first hexameric aryloxide aggregate where the metal is trisolvated.^{1,9} These K-O_{Diox} interactions may help weaken the K-O_{Ar} interaction. In the rubidium analogue, **6.3**, these two outer edges are only slightly longer (3.193 Å) than the other Rb-O_{Ar} distances, which have a range of 2.737(4) – 2.847(4) Å and a mean of 2.805 Å. There is one other hexameric structure that has the same open aggregate bonding as **6.2**, which is the pyridine solvate of potassium 2-methylphenoxide.⁹ Interestingly, the structure has two hexameric aggregates in the asymmetric unit that are both tetrasolvated by pyridine. The first aggregate has the same bonding as **6.2** with the two open edges on the corners, while the second aggregate has the commonly seen closed triple-stack of dimers motif.

The second major difference between the molecular structure of **6.1** and **6.2**, is that the potassium centers in **6.2** no longer have additional halide interactions. The potassiums in both of the complexes are coordinated by the same number of Lewis bases, however in **6.1** four of the potassiums have a K-F_{Ar} interaction, but in **6.4** this coordination has been replaced by dioxane. Therefore, there are still three different coordination environments for the potassiums, but now K1 is coordinated by two dioxanes, K2 by one dioxane, and K3 is coordinated by three dioxanes, for a total of twelve dioxanes solvating the aggregate. Since potassium (and sodium in the previous work) does not form a strong K-X_{Ar} interaction with any of the halides except fluoride, an argument could be made that the high electronegativity of the fluoride promotes these interactions.

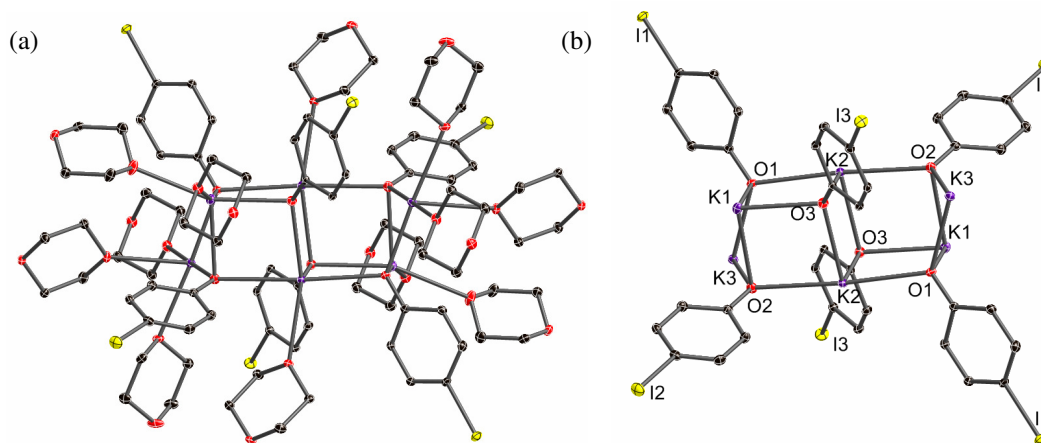


Figure 6.4 Structure of **6.2** showing (a) the full hexameric aggregate with twelve coordinated dioxane molecules, and (b) the hexameric aggregate with dioxane molecules removed for clarity.

6.2.3 Extended Structures

With all eight dioxanes bridging to other aggregates, plus the eight transannular K-F_{Ar} interactions, the hexameric aggregate in **6.1** has 16 connections to other aggregates

(Figure 6.5a,b). However, the aggregate is only an eight-connected node because it connects to every neighboring aggregate through double bridges (Figure 6.5c). There are three different types of double bridges between aggregates. The first type is the double dioxane bridge, which has been seen before in complexes highlighted in Chapters 4 and 5. This type of bridge accounts for two of the total points of extension. The second type of double bridge is the mixed dioxane and transannular K-F_{Ar} bridge, which accounts for four of the total points of extension. An example of this type of bridge can be seen with F3 coordinating to K3 of a neighboring aggregate while the dioxane molecule coordinated to K2 bridges to K2 of the same neighboring aggregate. The third type of double bridge, which accounts for two of the total points of extension, is the double K-F_{Ar} bridge. This bridge is seen with K1 (of aggregate “A”) coordinated by F2 from a neighboring aggregate (“B”) while F2 of aggregate “A” coordinates to K1 of aggregate “B”. Interestingly, the O1 aryloxy group is the only part of the aggregate not involved in transaggregate bonding.

Although the bridging between aggregates is rather unique, the eight-connected node gives an extended structure with **bcu** topology. This topology has now been seen multiple times in our own work and in others.¹⁰

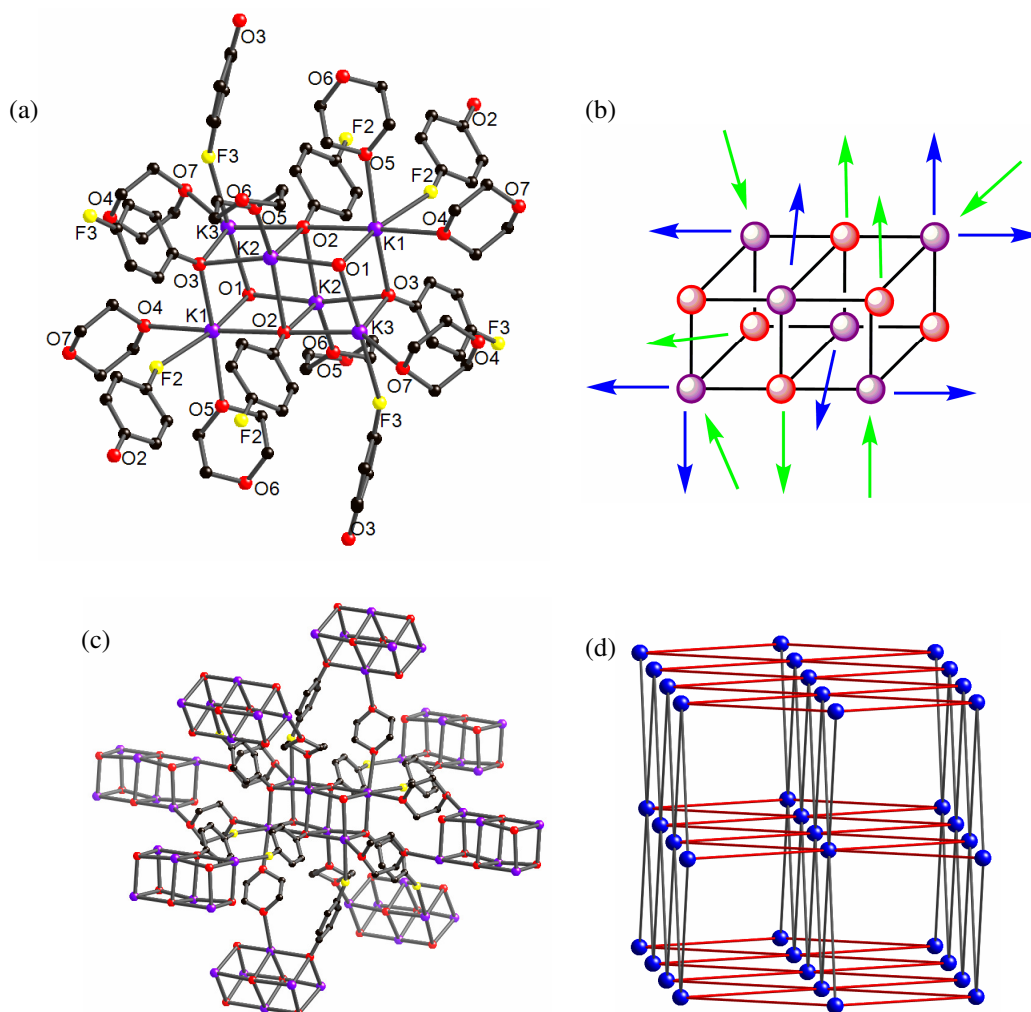


Figure 6.5 Structure of **6.1** showing (a) the hexameric aggregate with the eight bridging dioxanes shown as well as the eight aryloxy ligands that bridge through K-F_{Ar} interactions. (b) Illustration of the aggregate showing the eight bridging dioxane (blue arrows) and eight bridging aryl ligands (green arrows). (c) The hexameric aggregate bridged to neighboring aggregates through 8 double bridges. (d) The extended structure with **bcu** topology. The hexameric aggregates are shown as blue spheres and both types of bridges are shown as sticks.

Since **6.2** and **6.3** are isostructural, only the extended framework of **6.3** will be highlighted. The hexameric aggregate is coordinated by a total of twelve dioxane molecules (Figure 6.6a,b). However, the aggregate is only linked to six neighboring aggregates because each link is formed through a dioxane double bridge. To highlight

one of the double bridges, Rb3 and Rb1 bridge through dioxane to Rb2 and Rb3, respectively, of a neighboring aggregate. This is the first of our extended framework structures that is linked solely through the double dioxane bridge motif.

The 6-connected extended structure of **6.3** forms an extended structure with primitive cubic (**pcu**) topology. Surprisingly, there are only a few other complexes presented in this manuscript (**5.4**, **5.5**, **5.6**) that have **pcu** topology. This is unusual because of the common formation of the **pcu** net during our previous work with sodium aryloxides¹ and the frequent formation of this net topology in transition metal chemistry.⁴ As was mentioned in Chapter 4, the 6-connected **pcu** net is the second most common type of net, with 12.9% of all three-dimensional nets having this topology.⁴

The introductions in Chapters 4 and 5 discussed how smaller aggregates may be well suited to form high-connectivity nets because of the decrease in steric hindrance from the aryloxide groups. This was shown to be true with formation of the 7-connected networks. This argument for smaller aggregates is further strengthened by the characterization of **6.1-6.3**. All three hexameric aggregates have either sixteen or twelve points of network extension, but only form an 8- or 6-connected nets because of the formation of the double bridges. With the larger hexameric aggregate it becomes increasingly difficult to bridge to a high number of other aggregates, so the formation of the double bridge occurs.

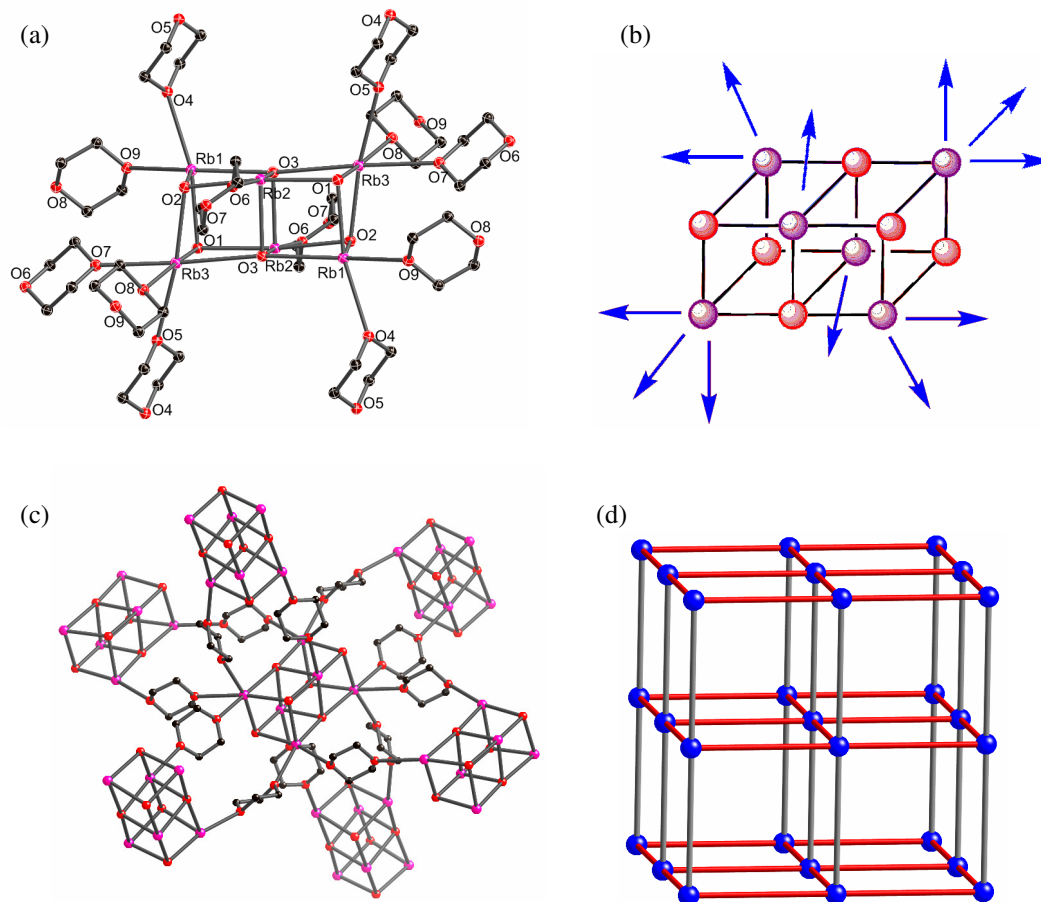


Figure 6.6 Structure of **6.3** showing (a) the hexameric aggregate coordinated by 12 bridging dioxane molecules. The carbon atoms of the aryloxy are removed for clarity. (b) Illustration of the aggregate showing the twelve bridging dioxanes (blue arrows). (c) The hexameric aggregate bridged to neighboring aggregates through 6 dioxane double bridges. (d) The extended structure with **pcu** topology. The hexameric aggregates are shown as blue spheres and dioxanes are shown as red and grey sticks.

6.3 Coordination Frameworks Built From Inorganic Rods

6.3.1 Synthesis

The equimolar reaction of 4-Cl-phenol or 4-Br-phenol with KHMDS or $[\text{RbO}^t\text{Bu} \cdot \text{Bu}^t\text{OH}]_\infty$ in 1,4-dioxane resulted in the instant formation of a precipitate, which dissolved on vigorous heating. High-quality crystals of both [(4-Cl-

$\text{C}_6\text{H}_4\text{OK})_3\cdot(\text{dioxane})_1]_\infty$ (**6.4**), $[(4\text{-Br-C}_6\text{H}_4\text{OK})_2\cdot(\text{dioxane})_{0.5}]_\infty$ (**6.5**), and $[(4\text{-Br-C}_6\text{H}_4\text{ORb})_5\cdot(\text{dioxane})_5]_\infty$ (**6.6**) were grown from the reaction solution after optimizing their concentrations and temperatures for crystal growth. Subsequent equimolar reactions of 4-*i*-Pr-phenol with KHMDS under similar crystallization conditions gave high-quality crystals of $[(4\text{-}^i\text{Pr-C}_6\text{H}_4\text{OK})_2\cdot(\text{dioxane})_{0.5}]_\infty$ (**6.7**).

6.3.2 Structures

The asymmetric unit of $[(4\text{-Cl-C}_6\text{H}_4\text{OK})_3\cdot(\text{dioxane})_1]_\infty$ (**6.4**) is composed of a potassium 4-bromophenoxide trimer where two of the potassium atoms are coordinated by a dioxane molecule. Symmetry expansion of the asymmetric shows that the potassium aryloxide does not form a discrete SBU, but rather an inorganic rod built from K-O_{Ar} interactions (Figure 6.7a,b). There are two different bonding environments for the potassiums. Both K1 and K2 are coordinated by one molecule of dioxane, as well as two μ_2 -aryloxide oxygen atoms and one μ_4 -aryloxide oxygen. The potassium in the middle of the inorganic rod, K3, is pseudo-octahedrally coordinated by two μ_4 -aryloxide oxygen atoms and four μ_2 -aryloxide oxygen atoms. Interestingly, there is significant differences in the K-O_{Ar} bond distances around K3. On one face of the octahedron there are three short K-O_{Ar} bond distances that range between 2.668(3) – 2.702(3) Å and on the face there are three long longer K-O_{Ar} bond distances of 2.791(3) – 2.877(3) Å.

Each inorganic rod is linked to four other rods through dioxane bridges to give an extended structure that resembles parallel stacks of 4⁴-nets (Figure 6.7c). Using the nomenclature discussed in the introduction, the net could be described as having I¹O²

topology since there is one direction of network growth with the inorganic rod and two directions of network growth with the bridging dioxane molecules.

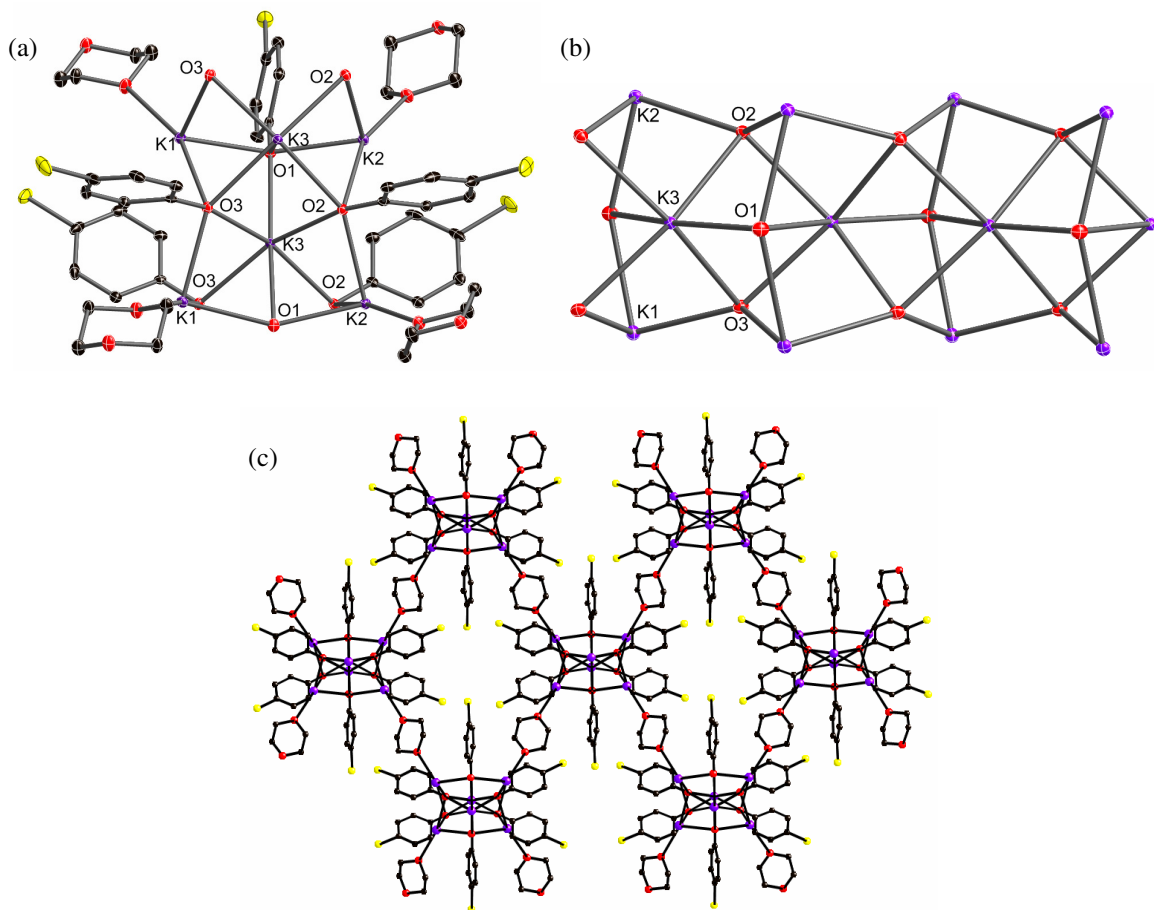


Figure 6.7 (a) Structure of **6.4** showing a slice of the extended inorganic structure formed through K-O_{Ar} interactions. (b) Simplified view of the inorganic chain showing only the K-O_{Ar} interactions. (c) Expanded view of the extended structure showing the inorganic rods bridged by dioxanes to give parallel stacks of 4⁴-nets.

The formation of the inorganic rod structure was completely unexpected since all of the sodium analogues of the 4-halo-aryloxides formed discrete SBUs. Moreover, all of the alkali metal aryloxide complexes our group has synthesized to date have formed discrete SBUs coordinated by a Lewis base, except for the cesium 4-Cl-2,6-dimethylphenoxide structure, **4.7**, which had no coordinated dioxane. Therefore, **6.4** falls

into a class of compounds that is a hybrid between inorganic extended structures and traditional metal-organic frameworks.

Synthesis of the potassium 4-bromophenoxide analogue, $[(4\text{-Br-C}_6\text{H}_4\text{OK})_2\cdot(\text{dioxane})_{0.5}]_\infty$ (**6.5**), yielded a complex very similar to **6.4**. In addition, a series of experiments was carried out to crystallize potassium 4-R-phenoxide dioxane complexes, where R = Me, ⁱPr, ^tBu, ^tPn, Ph. All of these experiments failed to produce crystalline materials except the isopropyl analogue, $[(4\text{-}^i\text{Pr-C}_6\text{H}_4\text{OK})_2\cdot(\text{dioxane})_{0.5}]_\infty$ (**6.7**). The complex is included in the series presented here because it is isostructural to **6.5**. As such, only **6.5** will be discussed further.

The asymmetric unit of **6.5** is composed of a potassium 4-Br-phenoxide dimer where one of the potassium atoms (K2) is coordinated by a molecule of dioxane. Symmetry expansion gives an extended structure similar to **6.4**. The only difference is there are three unique potassium environments in **6.4** (space group $P2_1/c$) and two unique potassium environments in **6.5** (space group $Pnma$). In **6.5**, K1 is the potassium atom that is in the middle of the inorganic rod and is pseudo-octahedrally coordinated by only aryloxy anions, while K2 is on both edges of the rod, and is coordinated by both dioxane and three aryloxy anions (Figure 6.8). Once again, the central potassium, K1, has both three short K-O_{Ar} bond distances of 2.675(2) - 2.685(2) Å and three long K-O_{Ar} distances of 2.816(2) - 2.866(2) Å. Since **6.5** is isostructural to **6.4**, the extended structure is the same as seen in Figure 6.7 with a one-dimensional inorganic rod that is connected to four other rods through dioxane bridges.

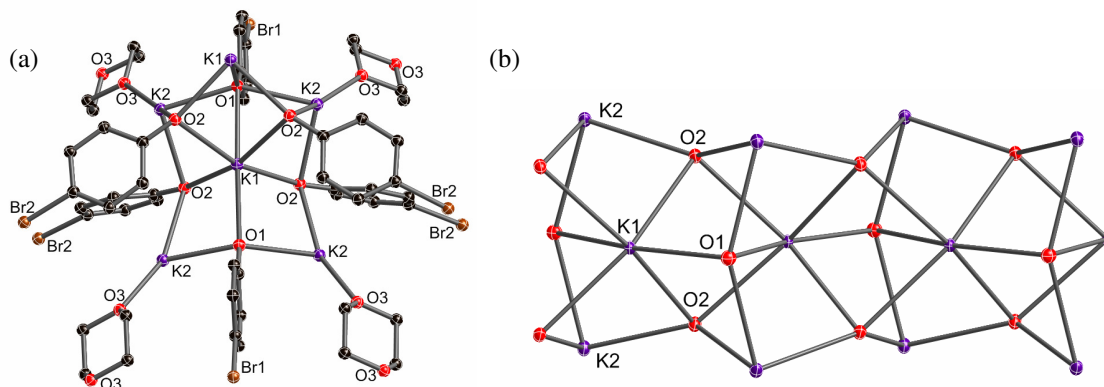


Figure 6.8 (a) Structure of **6.4** showing a slice of the extended inorganic structure formed through K-O_{Ar} interactions. (b) Simplified view of the inorganic chain showing only the K-O_{Ar} interactions.

The rubidium analogue of 4-Br-phenoxide, [(4-Br-C₆H₄ORb)₅·(dioxane)₅]_∞ (**6.6**), is composed of a rubidium aryloxy pentamer that is coordinated by dioxane. Symmetry expansion of the asymmetric unit once again gives a complex that does not form a discrete SBU but rather an inorganic rod built from Rb-O_{Ar} interactions (Figure 6.9a). All of aryloxy oxygen atoms in the structure are μ₄-bridges. There are three different bonding environments for the five rubidium centers. All of them are coordinated by four μ₄-aryloxy oxygen atoms but the dioxane coordination changes between the metals. In fact, there are two types of coordinated dioxane in the structure. In the first, the oxygen of the dioxane coordinates to one metal with a μ₁-interaction. In the second type of coordinated dioxane, the oxygen of the dioxane bridges between two metals as a μ₂-bridge (Figure 6.9b). This type of μ₂-bridge has been seen numerous times for THF solvated complexes.¹¹ In terms of the rubidium environments, both Rb1 and Rb5 are coordinated by one μ₂-dioxane, while Rb2 and Rb3 are coordinated by one μ₁-dioxane and one μ₂-dioxane, and Rb4 is coordinated by two μ₂-dioxane molecules.

The extended structure of **6.6** is composed of an inorganic rod that is built up through Rb-O_{Ar} interactions. Unlike the extended inorganic rods of **6.4**, **6.5**, and **6.7**, the inorganic rods of **6.6** are not bridged through dioxane (Figure 6.9d). Although all five rubidium centers are coordinated by dioxane, all of the dioxanes are terminal, which gives isolated inorganic rods. In this sense, **6.6** is very much like the cesium 4-Cl-2,6-dimethylphenoxide structure (**4.7**) that is built up through only Cs-O_{Ar} interactions. Each of the isolated inorganic rods are surrounded by six other rods in a hexagonal packing array. The closest possible interactions between rods are Rb-Br_{Ar} interactions, which are still 4.080 Å at the closest contact. As a point of reference, there are five structures in the CSD that have Rb-Br interactions that are less than the sum of the ionic radii (3.69 Å) and those distances range from 3.330 – 3.657 Å.¹² In terms of the nomenclature discussed in the introduction, the inorganic rods would be classified as a I¹O⁰ structure. One final note of interest is that the rods are helical as shown in Figure 6.9c, even though the space group is *P* 2₁/*c* since the rods in the extended structure have alternating handedness. The rod shown in Figure 6.9c has a left-handed helical twist.

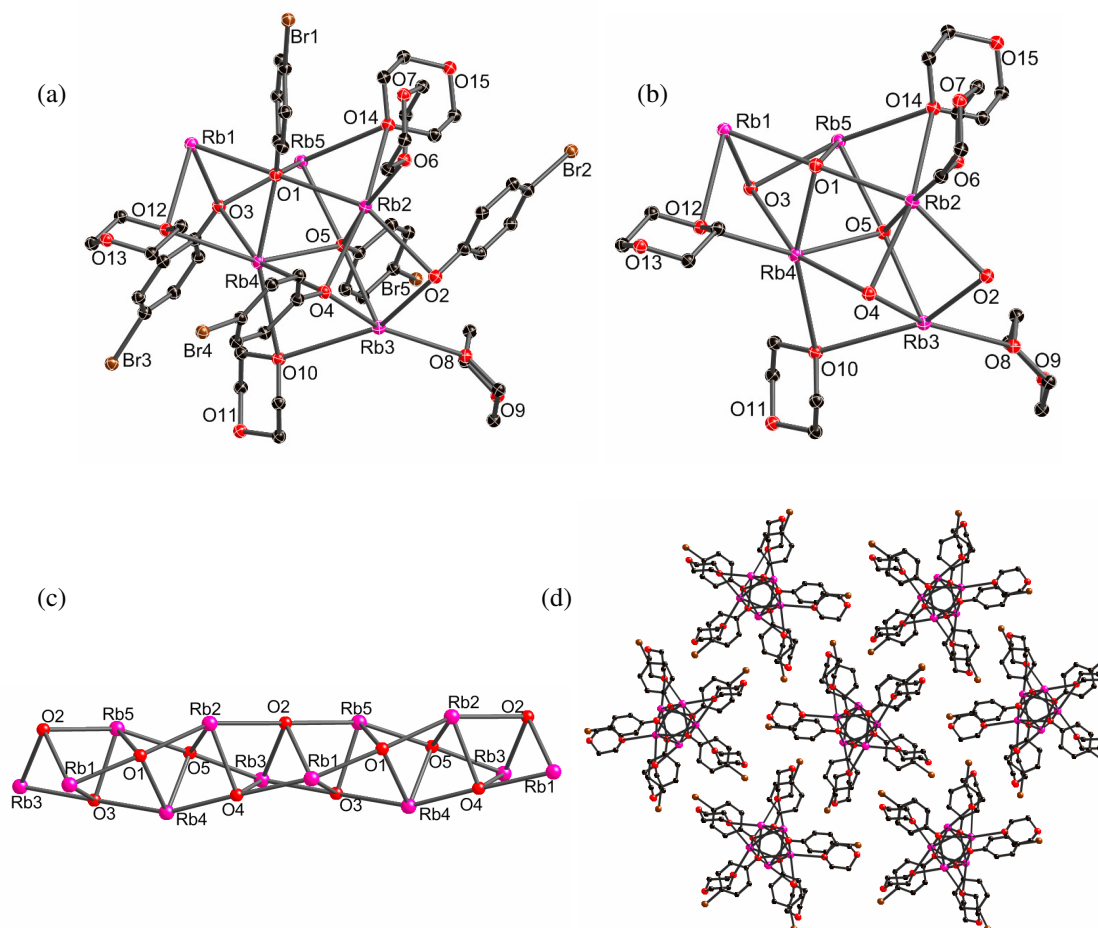


Figure 6.9 (a) Structure of **6.6** showing a slice of the extended inorganic structure formed through K-O_{Ar} interactions. (b) Simplified view of the inorganic chain showing only the K-O_{Ar} and K-O_{diox} interactions. (c) View of the K-O_{Ar} inorganic chain highlighting the helical structure. (d) Expanded view of the extended structure showing the isolated inorganic rods.

TABLE 6.1

KEY BONDS LENGTHS [\AA] AND ANGLES ($^\circ$) FOR **6.1-6.7**. MEAN PARAMETERS ARE IN BRACKETS

	M-O_{Ar}	M-O_{Dioxane}	O_{Ar}-M-O_{Ar}	M-O_{Ar}-M
6.1 (M=K)	2.5997(7) – 2.8602(7) <2.7129>	2.7021(8) – 2.7656(9) <2.7244>	84.10(2) – 168.99(2) <95.43>	85.12(2) – 175.41(3) <98.04>
6.2 (M=K)	2.623(1) – 2.895(1) <2.711>	2.781(1) – 2.831(1) <2.805>	82.27(2) – 175.18(4) <95.62>	91.14(4) – 113.18(5) <97.85>
6.3 (M=Rb)	2.737(4) – 3.193(4) <2.864>	2.855(4) – 2.997(5) <2.928>	77.45(12) – 172.45(12) <92.89>	88.55(15) – 173.73(15) <101.33>
6.4 (M=K)	2.668(3) – 2.812(3) <2.737>	2.682(3)	77.49(10) – 161.64(11) <98.75>	77.67(9) – 152.53(15) <104.28>
6.5 (M=K)	2.675(2) – 2.866(2) <2.755>	2.695(1)	73.51(4) – 161.09(3) <102.01>	75.74(3) – 149.51(8) <99.66>
6.6 (M=Rb)	2.774(3) – 3.016(3) <2.899>	3.089(4) – 3.329(3) <3.209>	70.05(9) – 162.22(9) <93.20>	82.09(8) – 173.3(1) <102.2>
6.7 (M=K)	2.673(1) – 2.909(1) <2.783>	2.8425(8)	72.51(2) – 161.77(4) <100.74>	74.18(2) – 152.08(3) <99.57>

6.4 Summary

The characterization of the *para*-substituted aryloxide aggregates, **6.1-6.7**, demonstrate that this class of compounds can readily be used as SBUs in the synthesis of extended coordination frameworks. Furthermore, the extended structures are constructed from two unusual types of interactions. Along with dioxane bridges, the three-dimensional structure of **6.1** forms strong K-F_{Ar} interactions, while the extended structures of **6.4-6.6** are composed of inorganic rods built from M-O-M interactions that are then cross-linked by bridging dioxane molecules. The types of interactions seen in **6.1-6.7** opens an area of new chemical and structural permutations that may be possible for extended structures built from alkali metal aggregates.

The work presented in the previous three chapters has shown there is a real paradigm shift between using transitional metals and the heavier alkali metals in the synthesis of extended materials. Transition metals, both isolated and as clusters, regularly give networks with high-symmetry and low-connectivity topologies. In contrast, the synthesized alkali metal aryloxide aggregates have given multiple examples of low-symmetry extended networks that are mainly highly connected. It is more surprising for these systems to give an extended structure with one of the common topologies like **dia** or **pcu**. For example, the only complexes in this entire work that have **pcu** topology are the isostructural **6.2** and **6.3**.

6.5 Experimental Section

6.5.1 General Procedures

All experimental manipulations were performed under a dry nitrogen atmosphere using standard Schlenk techniques, or in an argon-filled glovebox.¹³ All glassware was flame-dried under vacuum before use. Hexane was dried immediately before use by passage through columns of copper-based catalyst and alumina (Innovative Technology), and stored over 4 Å molecular sieves. Dioxane was purchased from Acros and was distilled over sodium benzophenone under N₂ prior to use. The phenols were purchased from Aldrich and were recrystallized from hexane. KHMDS was purchased from Aldrich and was used as received. [RbOBu^t·Bu^tOH]_∞, was prepared by literature methods.¹⁴ Deuterated solvents were purchased from Cambridge Isotope Laboratories and were dried by storage over 4 Å molecular sieves. ¹H and ¹³C NMR spectra were recorded on a Bruker AVANCE DPX-400 spectrometer at 293 K, and were referenced internally to the residual signals of the deuterated solvents.

6.5.2 X-ray Crystallography

Crystals were examined under Infineum V8512 oil. The datum crystal was affixed to a thin glass fibre mounted atop a tapered copper mounting-pin and transferred to the 100 K nitrogen stream of a Bruker APEX II diffractometer equipped with an Oxford Cryosystems 700 series low-temperature apparatus. Cell parameters were determined using reflections harvested from three sets of 20 0.3° ω scans. The orientation matrix derived from this was passed to COSMO to determine the optimum data collection strategy.¹⁵ Cell parameters were refined using reflections with $I \geq 10\sigma(I)$ harvested from

the entire data collection. All data were corrected for Lorentz and polarization effects, as well as for absorption. Tables A.8 and A.9 list the key crystallographic parameters for **6.1-6.7**. The structures were solved and refined using SHELXTL.¹⁶ Structure solution was by direct methods. Non-hydrogen atoms not present in the direct methods solution were located by successive cycles of full-matrix least-squares refinement on F^2 . All non-hydrogen atoms were refined with parameters for anisotropic thermal motion. Hydrogen atoms were placed at idealized geometries and allowed to ride on the position of the parent atom. Hydrogen thermal parameters were set to 1.2× the equivalent isotropic U of the parent atom, 1.5× for methyl hydrogens.

6.5.3 Preparation and Characterization

6.1 [(4-F-C₆H₄OK)₆·(dioxane)₄]_∞ - KHMDS (3 mmol, 598 mg) was added to a stirred solution of 4-F-phenol (3 mmol, 340 mg) in dioxane (20 mL). A white precipitate formed, which completely dissolved on heating the solution to reflux. X-ray quality crystals were obtained by slowly cooling the resulting solution in a hot water bath. ¹H NMR shows 0.15 equivalents of dioxane relative to the phenoxide, not 0.67 equivalents as in the crystal structure. Crystalline yield: 0.09 g, 69.2%. δ_{H} (*d*₆-DMSO, 293K) 3.56 (s, 7.2H, CH₂, dioxane), 5.98 (triplet, ⁴J_{H,F} = 8.0 Hz, 12H, *o*-H, Ar), 6.49 (dd, ³J_{H,F} = 8.0 Hz, 12H, *m*-H, Ar).

6.2 [(4-I-C₆H₄OK)₆·(dioxane)₆]_∞ - KHMDS (3 mmol, 598 mg) was added to a stirred solution of 4-I-phenol (3 mmol, 660 mg) in dioxane (16 mL). A white precipitate formed, which completely dissolved on heating the solution to reflux. X-ray quality crystals were obtained by slowly cooling the resulting solution in a hot water bath. ¹H

NMR shows 0.35 equivalents of dioxane relative to the phenoxide, not 1 equivalent as in the crystal structure. Crystalline yield: 0.22 g, 60.1%. δ_{H} (d_6 -DMSO, 293K) 3.56 (s, 16.7H, CH₂, dioxane), 5.86 (doublet, $^3J_{\text{H,H}} = 8.0$ Hz, 12H, *o*-H, Ar), 6.83 (doublet, $^3J_{\text{H,H}} = 8.0$ Hz, 12H, *m*-H, Ar).

6.3 [(4-I-C₆H₄ORb)₆·(dioxane)₆]_∞ - [RbOBu^t·Bu^tOH]_∞ (1 mmol, 230 mg) was added to a stirred solution of 4-I-phenol (1 mmol, 220 mg) in dioxane (9 mL). A white precipitate formed, which completely dissolved on heating the solution to reflux. X-ray quality crystals were obtained by slowly cooling the resulting solution in a hot water bath. ¹H NMR shows 2.2 equivalents of dioxane relative to the phenoxide, not 1 equivalent as in the crystal structure. δ_{H} (d_6 -DMSO, 293K) 3.56 (s, 106H, CH₂, dioxane), 5.84 (doublet, $^3J_{\text{H,H}} = 8.0$ Hz, 12H, *o*-H, Ar), 6.80 (doublet, $^3J_{\text{H,H}} = 8.0$ Hz, 12H, *m*-H, Ar).

6.4 [(4-Cl-C₆H₄OK)₃·(dioxane)]_∞ - KHMDs (3 mmol, 598 mg) was added to a stirred solution of 4-Cl-phenol (3 mmol, 390 mg) in dioxane (10 mL). A white precipitate formed, which completely dissolved on heating the solution to reflux. X-ray quality crystals were obtained by slowly cooling the resulting solution in a hot water bath. Crystalline yield: 0.48 g, 81.8 %. δ_{H} (d_6 -DMSO, 293K) 3.56 (s, 8H, CH₂, dioxane), 5.94 (doublet, $^3J_{\text{H,H}} = 8.0$ Hz, 6H, *o*-H, Ar), 6.55 (doublet, $^3J_{\text{H,H}} = 8.0$ Hz, 6H, *m*-H, Ar).

6.5 [(4-Br-C₆H₄OK)₂·(dioxane)_{0.5}]_∞ - KHMDs (3 mmol, 598 mg) was added to a stirred solution of 4-Br-phenol (3 mmol, 520 mg) in dioxane (15 mL). A white precipitate formed, which completely dissolved on heating the solution to reflux. X-ray quality crystals were obtained by slowly cooling the resulting solution in a hot water bath. Crystalline yield: 0.25 g, 32.9%. δ_{H} (d_6 -DMSO, 293K) 3.56 (s, 4H, CH₂, dioxane), 5.92 (doublet, $^3J_{\text{H,H}} = 8.0$ Hz, 4H, *o*-H, Ar), 6.69 (doublet, $^3J_{\text{H,H}} = 8.0$ Hz, 4H, *m*-H, Ar).

6.6 [(4-Br-C₆H₄ORb)₅·(dioxane)₅]_∞ - [RbOBu^t·Bu^tOH]_∞ (1 mmol, 230 mg) was added to a stirred solution of 4-Br-phenol (1 mmol, 173 mg) in dioxane (14 mL) and hexane (14 mL). A white precipitate formed, which completely dissolved on heating the solution to reflux. X-ray quality crystals were obtained by slowly cooling the resulting solution in a hot water bath. Crystalline yield: 0.15 g, 43.5 %. δ_{H} (*d*₆-DMSO, 293K) 3.56 (s, 40H, CH₂, dioxane), 5.88 (doublet, ³J_{H,H} = 8.0 Hz, 10H, *o*-H, Ar), 6.28 (doublet, ³J_{H,H} = 8.0 Hz, 10H, *m*-H, Ar).

6.7 [(4-ⁱPr-C₆H₄OK)₂·(dioxane)_{0.5}]_∞ - KHMDs (3 mmol, 598 mg) was added to a stirred solution of 4-ⁱPr-phenol (3 mmol, 409 mg) in dioxane (7 mL) and hexane (5 mL). A white precipitate formed, which completely dissolved on heating the solution to reflux. X-ray quality crystals were obtained by slowly cooling the resulting solution in a hot water bath. ¹H NMR shows 0.15 equivalents of dioxane relative to the phenoxide, not 0.25 equivalents as in the crystal structure. Crystalline yield: 0.28 g, 79.3%. δ_{H} (*d*₆-DMSO, 293K) 1.09 (s, 18H, CH(CH₃)₂), 3.07 (multiplet, ³J_{H,H} = 8.0 Hz 4H, CH(CH₃)₂), 3.56 (s, 2.5H, CH₂, dioxane), 6.08 (doublet, ³J_{H,H} = 8.0 Hz, 4H, *o*-H, Ar), 6.65 (doublet, ³J_{H,H} = 8.0 Hz, 4H, *m*-H, Ar).

6.6 References

- [1] MacDougall, D. J.; Noll, B. C.; Henderson, K. W. *Inorg. Chem.* **2005**, *44*, 1181.
- [2] (a) MacDougall, D. J.; Morris, J. J.; Noll, B. C.; Henderson, K. W. *Chem. Commun.* **2005**, 456. (b) Morris, J. J.; Noll, B. C.; Henderson, K. W. *Cryst. Growth Des.* **2006**, *6*, 1071. (c) Morris, J. J.; Noll, B. C.; Honeyman, G. G.; Kennedy, A. R.; Mulvey, R. E.; Henderson, K. W. *Chem. –Eur. J.* **2007**, *13*, 4418. (d) Morris, J. J.; Noll, B. C.; Henderson, K. W. *Chem. Commun.* **2007**, 5191. (e) Morris, J. J.; Noll, B. C.; Schultz, A. J.; Piccoli, P. M. B.; Henderson, K. W. *Inorg. Chem.* **2007**, *46*, 10473.

- [3] Cheetham, A. K.; Rao, C. N. R.; Feller, R. K. *Chem. Commun.* **2006**, 4780.
- [4] Ockwig, N. W.; Delgado-Friedrichs, O.; O’Keeffe, M.; Yaghi, O. M. *Acc. Chem. Res.* **2005**, *38*, 176.
- [5] Rosi, N. L.; Kim, J.; Eddaoudi, M.; Chen, B.; O’Keeffe, M.; Yaghi, O. M. *J. Am. Chem. Soc.* **2005**, *127*, 1504.
- [6] Guillou, N.; Livage, C.; van Beek, W.; Nogues, M.; Férey, G. *Angew. Chem., Int. Ed.* **2003**, *42*, 644.
- [7] Feller, R. K.; Cheetham, A. K. *Solid State Sci.* **2006**, *8*, 1121.
- [8] Allen, F. H. *Acta Cryst.* **2002**, *B58*, 380.
- [9] Boyle, T. J.; Andrews, N. L.; Rodriguez, M. A.; Campana, C.; Yiu, T. *Inorg. Chem.* **2003**, *42*, 5357.
- [10] (a) Long, D. -L.; Blake, A. J.; Champness, N. R.; Wilson, C.; Schröder, M. *Angew. Chem. Int. Ed.* **2001**, *40*, 2443. (b) Luo, T. -T.; Tsai, H. -L.; Yang, S. -L.; Liu, Y. -H.; Yadav, R. D.; Su, C. -C.; Ueng, C. -H.; Lin, L. -G.; Lu, K. -L. *Angew. Chem. Int. Ed.* **2005**, *44*, 6063. (c) Zhang, X. -M.; Fang R. -Q.; Wu, H. -S. *J. Am. Chem. Soc.* **2005**, *127*, 7670. (d) Li, D.; Wu, T.; Zhou, X. -P.; Zhou, R.; Huang, X. -C. *Angew. Chem. Int. Ed.* **2005**, *44*, 4175. (e) Fang, Q. -R.; Zhu, G. -S.; Jin, Z.; Xue, M.; Wei, X.; Wang, D. -J.; Qiu, S. -L. *Angew. Chem. Int. Ed.* **2006**, *45*, 6126. (f) Zhang, J.; Kang, Y.; Zhang, J.; Li, Z. -J.; Qin, Y. -Y.; Yao, Y. -G. *Eur. J. Inorg. Chem.* **2006**, 2253.
- [11] For a recent example see: Chivers, T.; Fedorchuk, C.; Parvez, M. *Inorg. Chem.* **2004**, *43*, 2643.
- [12] (a) Helgesson, G.; Jagner, S. *J. Chem. Soc., Dalton Trans.* **1993**, 1069. (b) Rusanova, J. A.; Domasevitch, K. V.; Vassilyeva, O. Y.; Kokozay, V. N.; Rusanov, E. B.; Nedelko, S. G.; Chukova, O. V.; Ahrens, B.; Raithby, P. R. *J. Chem. Soc., Dalton Trans.* **2000**, 2157. (c) Ahmad, R.; Hardie, M. J. *New. J. Chem.* **2004**, *28*, 1315. (d) Ahmad, R.; Franken, A.; Kennedy, J. D.; Hardie, M. J. *Chem. Eur. J.* **2004**, *10*, 2190. (e) Kitanovski, N.; Golic, L.; Meden, A.; Ceh, B. *Croat.Chem.Acta* **2005**, *78*, 111.
- [13] Schriver, D. F.; Drezdon, M. A. *The Manipulation of Air-Sensitive Compounds*, Wiley, New York, **1986**.

- [14] Chisholm, M. H.; Drake, S. R.; Nairni, A. A.; Streib, W. E. *Polyhedron* **1991**, *10*, 337.
- [15] J. Kaercher, *COSMO*, Bruker-Nonius AXS, Inc., Madison, Wisconsin, USA, **2003**.
- [16] G. M. Sheldrick, University of Göttingen, Göttingen (Germany), **2001**.